

THEORETICAL INVESTIGATION OF CORROSION OF MILD STEEL IN ACIDIC MEDIUM BY TRIAZOLE BASED SCHIFFS BASE AS INHIBITOR

R. SHANTHI^a AND R. JOEL KARUNAKARAN^{1b}

^{ab}Department of Chemistry, Madras Christian College, Tambaram, Chennai, India

ABSTRACT

The inhibitive performance of three triazoles namely diamino triazole (TA), anisaldine 3, 5-diaminotriazole (ATA), vanilidine 3,-diaminotriazole (VTA) have been studied using DFT approach. The inhibitors investigated in B3LYP/6-31G** level in non-protonated and protonated forms are successfully proven to inhibit the corrosion of mild steel in acidic medium in the order VTA>ATA > TA. This is found to be consistent with the reported inhibition efficiencies. The electrostatic potential diagram gives a better idea on the inhibition phenomenon.

KEYWORDS : Nitrogen based triazoles, Molecular orbital calculations, Corrosion inhibition

Inhibition of corrosion is an extensive field of research undertaken across the globe. The inhibition of corrosion is still more important as all the industrial process are dependent on acidic medium as acids are more aggressive medium that attacks the surface (Mu and Li, 2005). But the cost and time efforts that have been invested is huge when compared to the negligible out come obtained. But theoretical chemistry provides an alternative and easy route to assess the corrosion behavior of the molecule. The molecular properties of the inhibitor molecules can be correlated to their inhibition efficiencies by using the advanced molecular modelling techniques and quantum chemical calculations (Awad et al., 2010).

The inhibition of corrosion of mild steel in acidic medium has driven considerable interest because of its industrial applications. The inhibitor that contains hetero atom like nitrogen, oxygen, sulfur was found to show more of inhibition efficiency. Among these compounds nitrogen containing inhibitors especially triazoles have been investigated by (Abdelghani et al, 2007). Use of triazole and Schiff's base have been successfully proven to be good in inhibition of corrosion. Schiff's base containing polydentate ligand was also found to be providing encouraging results experimentally

The inhibition of corrosion not only depends on the nature of the medium. Several factors like structure of inhibitor, number of active centers in the inhibitor molecule, nature of metal surface, complex formed in the molecule, mode of adsorption taking place in the molecule also

determines the inhibition efficiency of the concerned molecule. The aim of the present study is to get a deep insight into the mechanism of corrosion through molecular orbital calculations. The active site for adsorption of the molecule have been found through single point energy calculations. The same is confirmed by using the electrostatic potential diagrams. Fig 1. indicates the structure of the investigated inhibitors: 3,5-diamino-1,2,4-triazole (TA), anisaldine-3,5-diamino-1,2,4-triazole (ATA), vanilidine-3,5-diamino-1,2,4-triazole (VTA).

Theory and Computational Methods

The structures of the investigated compounds are initially optimized using the semi-empirical AM1 method using Cs point group, agreed well with the experimental trend reported. Then the resultant structures were optimized using DFT method B3LYP employing Pople's 6-31G (d,p) split-valence basis set at the Restricted Hartree Fock level (RHF). All the optimizations were carried out using PC GAMESS/Firefly QC Packages (Alex. A. Granovsky) which is partially based on GAMESS(US) The optimized structure was visualized using McMolplt (Bode and Gordon, 1998) program. The electrostatic potential values are calculated using MULTIWFN software (Tian Lu and Feiwu Chen, 2012). The visualization of the electrostatic potential is done by using Jmol software (Jmol website).

¹Corresponding author

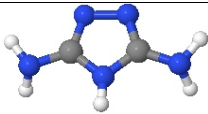
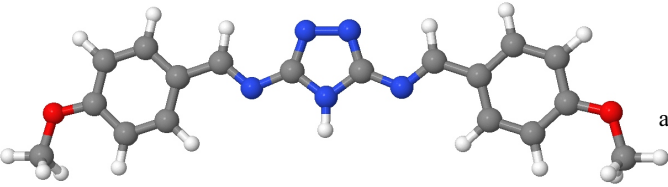
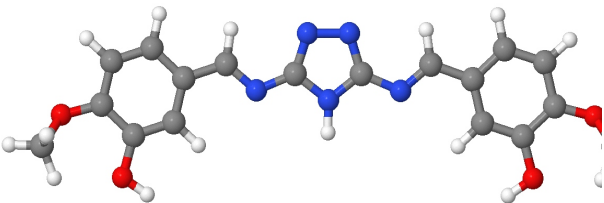
| Chemical structure | Name | Ab |
|---|---------------------------------------|-----|
|  | 3,5-diamino-1,2,4-triazole | TA |
|  | anisidine-3,5-diamino-1,2,4-triazole | ATA |
|  | vanilidine-3,5-diamino-1,2,4-triazole | VTA |

Fig. 1. Name, Molecular structure s of the inhibitors along with abbreviation.

The major quantum chemical parameters that can be correlated to the inhibition efficiency is the energies of highest occupied molecular orbital E_{HOMO} and the energy of lowest unoccupied molecular orbital E_{LUMO} . The total energy of the molecule (E_{tot}), band gap ($\Delta E = E_{\text{LUMO}} - E_{\text{HOMO}}$), the fraction of electrons transferred from the inhibitor to the metal (ΔN), dipole moment (μ) are calculated for the inhibitor molecule (Gece, 2008). The favorable position for adsorption in the inhibitor molecules could be predicted from the energies of frontier molecular orbital. Adsorption occurs preferably in the position where the softness value (σ) is highest. Softness is a local property. Koopmans theorem is helpful to relate the E_{HOMO} and E_{LUMO} of the inhibitor molecule to the ionization potential, I , and Electron affinity, A , using the Eq. (1)

$$I = -E_{\text{HOMO}}, A = -E_{\text{LUMO}} \quad (1)$$

The electronegativity χ and the absolute hardness η of the inhibitor molecule concerned is related by using the relationship given by (2)

$$\chi = \frac{I+A}{2} \text{ and } \eta = \frac{I-A}{2} \quad (2)$$

Based on the values of electronegativity and hardness the fraction of electron transferred to the metal from the inhibitor can be calculated by using Eq.3. The computational values of $\chi_{\text{Fe}} = 7.0 \text{ eV}$ and $\eta_{\text{Fe}} = 0$.

$$\Delta N = \frac{\chi_{\text{Fe}} - \chi_{\text{inh}}}{2(\eta_{\text{Fe}} + \eta_{\text{inh}})} \quad (3)$$

The space generated around a molecule by its nuclei and static distribution of electron is called as the electrostatic potential. The electrostatic potential is very much useful for predicting the reactivity of the molecule. The structure of metal bound to the inhibitor molecule has been optimized using Pople's split valence basis set 3-21G(d,p) at the Restricted Hartree Fock level (RHF) and the single point energy have been found out at the 6-31G (d,p) level using the DFT method B3LYP.

RESULTS AND DISCUSSION

The inhibition efficiency of 3, 5-diamino-1, 2, 4 triazole Schiff's base derivatives have been studied experimentally and it been proven that these inhibitors follow the trend $VTA > FTA > ATA > TA$ (Gopi et al., 2000). The experimental inhibition efficiency reported are 78.04, 86.24, 92.81 percentage respectively for TA, ATA, VTA respectively. The FTA molecule experimentally encountered is ignored in the present study. The high electron density of nitrogen atom of the C=N group of the Schiff's base structure also triggers up a high inhibition. The presence of non-bonding electrons in the sp^2 hybridized nitrogen atom and the π electron cloud in the triazole ring are responsible for the adsorption of the metal atom on the surface of the inhibitor in the parent molecule. It was found that the VTA molecule inhibits the corrosion more when compared to the other molecules considered. This may be because of the hydroxyl and methyl functional group attached to the benzene ring that helps in better adsorption and helpful in binding the non-bonding electrons found in vacant orbitals of the metal surface. A better donor acceptor link is very much helpful in increasing the binding ability. The inhibition efficiency is also dependent on the molecular size and structure of the inhibitor. An optimized electronic and molecular structure with minimum energy is obtained and their frontier molecular diagrams are given in Fig 2, 3. In the present case, Mulliken population analysis predicts that N4 is the most favorable position for getting protonated.

QUANTUM CHEMICAL PARAMETERS OF TRIAZOLE DERIVATIVES

All the three molecule encountered are planar and symmetric in nature. The parent molecule contains two nitrogen atoms and it has the lowest inhibition efficiency. On substitution of electron withdrawing OH and OCH_3 groups, the inhibition efficiency increases. The inhibition takes place in acidic medium. So the structure of protonated inhibitor is also encountered. All the data were compared in B3LYP/6-31G** level. According to the Frontier molecular orbital (FMO), the chemical reactivity of the molecule is determined by the E_{HOMO} and E_{LUMO} of the molecule concerned.

Hard molecules are the molecules that have a large separation energy gap. The inverse of hardness of the molecule (σ). In turn, soft molecules possess a smaller separation energy gap, as well as more reactive. Soft molecules are better electron donors, hence offers electrons to the metal surface easily. During the process of inhibition, the metal atom behaves like a Lewis acid and the inhibitor acts as Lewis base or a soft base.

The dipole moment of the molecule represents the variation of energy with the applied electric field. Dipole moment is the measure of polarity of a polar covalent bond. It is defined as the product of charge on the atoms and the bond length between atoms. The total dipole moment is the vector sum of individual bond dipole moments, measure of the global polarity of a molecule. The dipole moment is obtained from non-uniform distribution of charges on the various atoms in the molecule. The energy of the deformability, volume of the inhibitor molecules is directly proportional to dipole moment. This increases the contact area between the molecule and surface of metal and increasing the corrosion inhibition ability of inhibitors. The dipole moment of the inhibitor molecule cannot be related to the inhibition efficiency significantly. The inhibitor molecule can be adsorbed in three different ways. The neutral molecule or the protonated inhibitor can be involved in inhibition of corrosion. The electrostatic interaction between electron rich inhibitor and the electron deficit metal surface is also an alternative route way for the inhibition phenomenon.

As can be found in the Table 1 the energy E_{HOMO} of the molecule increases in the order $VTA > ATA > TA$ at the B3LYP/6-31G** level. Among the factors determined, E_{HOMO} and E_{LUMO} predicts the ability of the inhibitor molecule to donate its electron to the appropriate donor and accept the electrons respectively.

In general, the E_{HOMO} determined is related to the ionization potential (IP). Lower the ionization potential of molecule, higher is its inhibition efficiency. It is implicit that higher the value of E_{HOMO} , higher is the tendency of molecule to donate electron to appropriate donor. Lower the E_{LUMO} value higher is the capacity to accept electrons. When the E_{HOMO} is considered as the tool to decide the reactivity of the molecule, then it follows the order

Non-protonated: $VTA > ATA > TA$ E_{HOMO}

Protonated: $VTA > ATA > TA$ E_{HOMO}

Similarly, if the E_{LUMO} is the decisive factor then it can be arranged as

Non-protonated: VTA>ATA>TA E_{LUMO}

Protonated: VTA>ATA>TA E_{LUMO}

The separation energy is another factor that decides the inhibition efficiency of the molecule. The lower is the energy gap more is the inhibition efficiency. In the present cases the separation energy between VTA and ATA are almost similar in the non-protonated species. This is acceptable because the inhibition efficiencies determined experimentally are relatively close to each other. But in the protonated molecules the trend once again matches with the inhibition efficiency.

Protonated: VTA>ATA>TA ΔE

ΔN is the parameter that determines the number of electrons transferred from the inhibitor to the metal surface. Lukovits's study reveals that, if $\Delta N < 3.6$, molecules with increased electron donating ability has higher inhibition efficiency. The ΔN doesn't correspond to the exact number of electrons transferred from the inhibitor to the metal surface. In other words, it indicates the electron donating ability of the molecule. The electron donating ability of VTA molecule in both protonated and non-protonated level is found to be more than other species. If ΔN is the decisive factor, then the inhibition efficiency can be arranged as

Non-protonated: VTA>ATA>TA ΔN

Protonated: VTA>ATA>TA ΔN

According to Sanderson's electronegativity equalization principle, the molecule that has higher

electronegativity is having poor inhibition. If the electronegativity is the decisive factor then the trend follows the order.

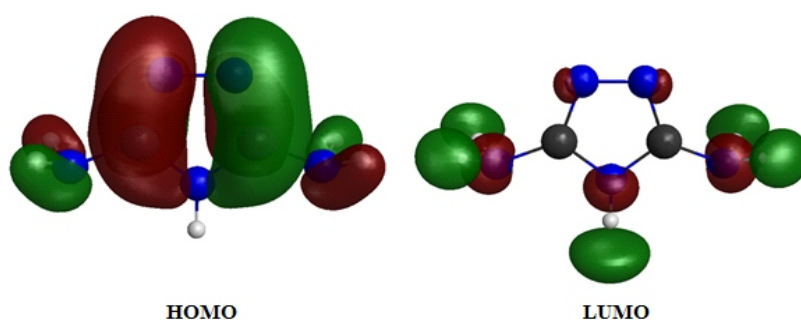
Protonated: VTA>ATA>TA χ

The absolute hardness of the molecule η signifies the resistance towards polarization of the molecule under small perturbation of the chemical reaction. The molecule that has large energy gap is hard and lower energy gap is soft. In this case the VTA molecule is soft and offers more electron to the acceptor molecule. The molecule with lower value of hardness and higher value of softness is found to be good. If softness of the molecule is the decisive factor then the trend follows

Protonated: VTA>ATA>TA σ

Relationship Between Surface Area, Volume And Inhibition Efficiency

The molecular volume and the surface area of the protonated and non-protonated inhibitor are tabulated in Table 3. Significant relationship between the molecular volume and inhibition efficiency have been established (Hasanov et al., 2007). The VTA molecule in the protonated form shows a maximum surface area. The molecule that has maximum surface area covers the metal better and the inhibitor-metal contact area increases. This leads to a better inhibition. Polarizability of the molecule increases with increase in molecular volume, which in turn increases adsorptive properties of both metals and the inhibitors.



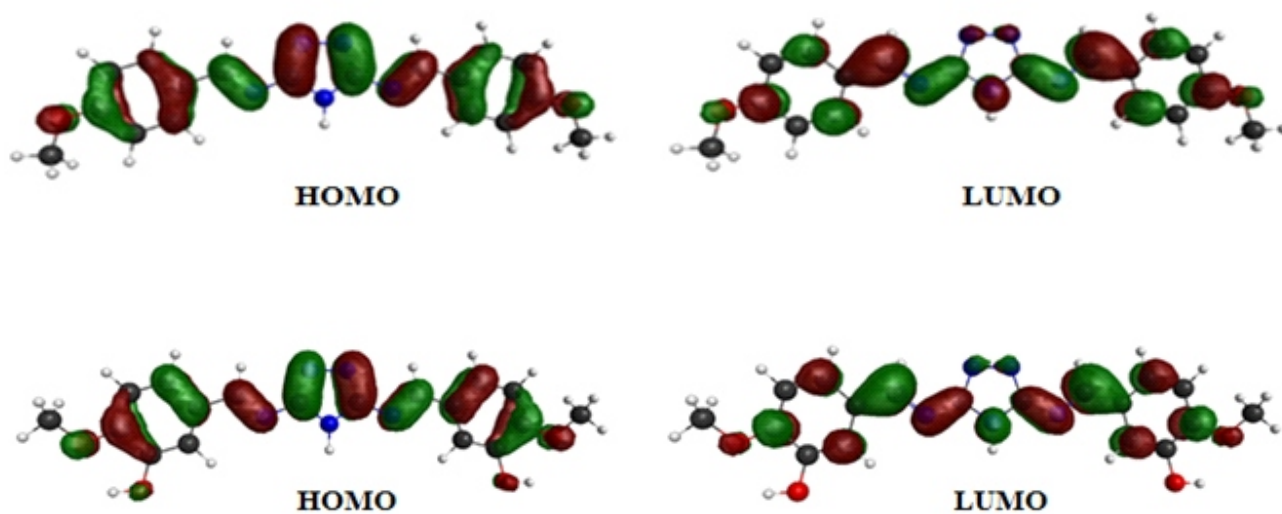


Fig. 2: HOMO-LUMO diagram of the neutral inhibitor

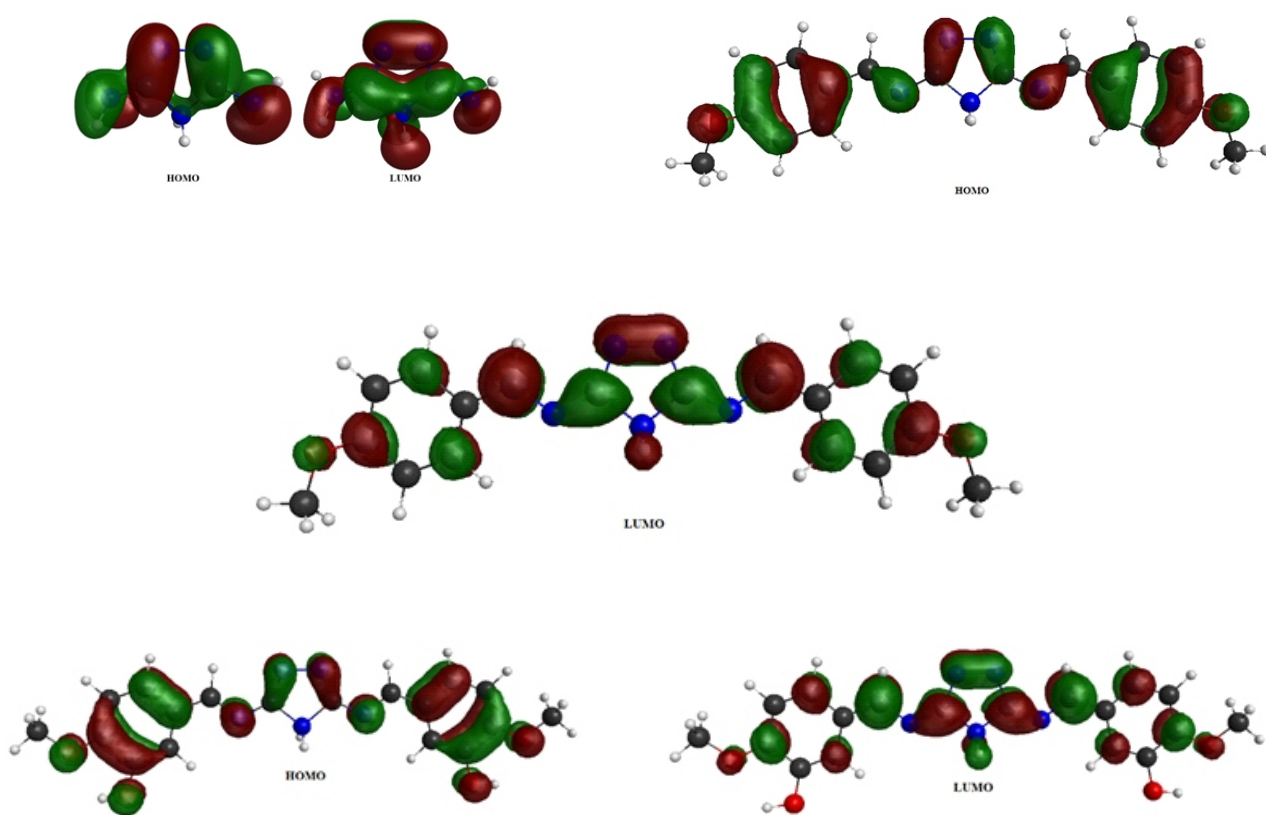


Fig. 3 : HOMO-LUMO diagram of the protonated inhibitor

There is a lack of agreement between the dipole moment (μ) of the molecule and the inhibition efficiency. All quantum chemical parameters of the protonated compounds were correlated against the experimental IE (%) values and the regression values (R^2) for each parameter corresponding to the method of calculations are shown in fig 4. Good correlations are found for E_{tot} , E_{LUMO} , ΔN parameters.

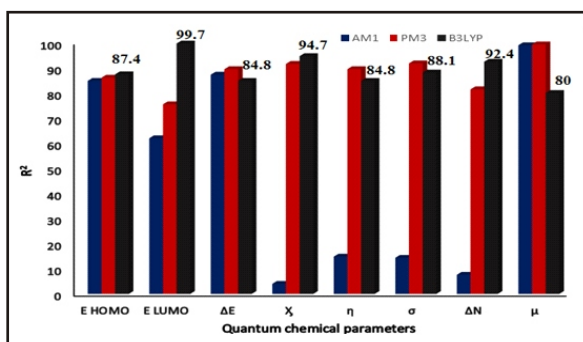


Fig. 4 : A plot of regression values (R^2) obtained from the correlation between the quantum chemical parameters and IE (%) for the protonated inhibitors

Role of Inhibitor in Binding with the Metal

Transition metals creates a lot of convergence problems as they are electron rich in nature. At the ab initio level the calculations are time consuming. Mulliken Population analysis method have been utilized to calculate the charge distribution on the whole skeleton of the molecule. The hetero atom with highest negative charge tend to be get adsorbed in the metal surface during the donor-acceptor mechanism in all the three inhibitors considered, N1 has the highest negative charge. The structure of the inhibitors bound to the surface were optimized in 3-21G** level and the single point energy was calculated in 6-31G** level. All the molecule considered has minimum energy if the molecule is bound to N1 (Table 4). This helps us to understand the feasible site of attack during the metal-inhibitor binding.

Electrostatic Potential Diagram

Electrostatic potential map are widely used to predict the interaction of charged species with other atom (Peter Politzer et al., 1995). The electrostatic potential map for all the three molecules have been given in fig 5. The

region with negative potential indicates the ease of particular site to undergo a nucleophilic attack. The negative potential is concentrated more on atoms N1 and N2 (Tian Lu and Feiwu Chen, 2012). The electrostatic potential calculations show that N1 has the highest value of calculated V_{min} , which indicates N1 is easily attached to Fe atom of the metal surface (Table.5)

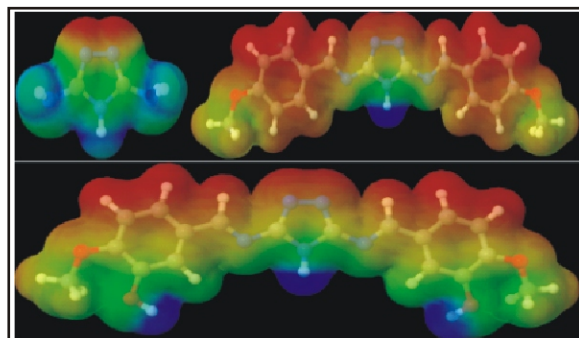


Fig. 5: Electrostatic potential contour diagram for the inhibitors with red color indicating the region with negative potential

CONCLUSION

Quantum chemical calculations in AM1, PM3, DFT/B3LYP level shows an agreement between quantum chemical parameters and the electronic structure of the molecule are clearly related to the inhibition process. The parameters E_{HOMO} , E_{LUMO} , ΔN shows a complete agreement with the experimental trend in both protonated and non-protonated conditions. The factors E_{HOMO} , E_{LUMO} , ΔN , ΔE , χ , σ shows a good agreement with the experiment in protonated form. The dipole moment (μ) of the molecule cannot be related to the inhibition efficiency. The volume of protonated VTA is maximum indicating that it possess highest inhibition efficiency. The single point energy calculations shows that, binding of the metal was found to take place in N1. The same is confirmed by the V_{min} values of the electrostatic potential.

Table 1: Calculated quantum chemical parameters for non-protonated inhibitors

| System | $-E_{\text{tot}}^*$ | E_{HOMO}^{**} | E_{LUMO}^{**} | ΔE^{**} | χ | η | σ | $\Delta N(e)$ | μ |
|--------------------|---------------------|------------------------|------------------------|-----------------|--------|---------|----------|---------------|-------|
| Semi empirical AM1 | | | | | | | | | |
| TA | 31315.556 | -0.3348 | 0.0149 | 0.3497 | 0.1600 | 0.1749 | 5.718 | 0.2774 | 3.061 |
| ATA | 96123.7333 | -0.3093 | -0.0351 | 0.2742 | 0.1722 | 0.1371 | 7.294 | 0.3102 | 4.716 |
| VTA | 111813.021 | -0.3116 | -0.0404 | 0.2712 | 0.1760 | 0.1356 | 7.375 | 0.2997 | 4.285 |
| Semi empirical PM3 | | | | | | | | | |
| TA | 25929.997 | -0.3630 | 0.0008 | 0.3638 | 0.1811 | 0.1819 | 5.498 | 0.2090 | 3.315 |
| ATA | 87398.143 | -0.3173 | -0.0390 | 0.2783 | 0.1392 | 0.1782 | 5.612 | 0.3314 | 4.791 |
| VTA | 100943.608 | -0.3272 | -0.0483 | 0.2789 | 0.1878 | 0.1395 | 7.168 | 0.2489 | 3.626 |
| B3LYP/6-31G** | | | | | | | | | |
| TA | 221501.806 | -0.2193 | -0.0276 | 0.1917 | 0.1235 | 0.09585 | 10.433 | 0.6977 | 4.352 |
| ATA | 703016.930 | -0.1945 | -0.0650 | 0.1295 | 0.1298 | 0.0648 | 15.432 | 0.9836 | 5.697 |
| VTA | 796973.168 | -0.1897 | -0.0601 | 0.1296 | 0.1249 | 0.0648 | 15.432 | 0.9849 | 0.182 |

* -kcalmol⁻¹, ** -a.u, *** -Debye**Table 2: Calculated quantum chemical parameters for protonated inhibitors**

| System | $-E_{\text{tot}}^*$ | E_{HOMO}^{**} | E_{LUMO}^{**} | ΔE^{**} | χ | η | σ | $\Delta N(e)$ | μ^{***} |
|--------------------|---------------------|------------------------|------------------------|-----------------|--------|--------|----------|---------------|-------------|
| Semi empirical AM1 | | | | | | | | | |
| TA | 31448.630 | -0.5230 | -0.2102 | 0.3128 | 0.3666 | 0.1564 | 6.394 | -0.3496 | 6.601 |
| ATA | 97226.872 | -0.4227 | -0.1964 | 0.2263 | 0.3096 | 0.1132 | 8.382 | -0.2312 | 4.211 |
| VTA | 112010.277 | -0.4160 | -0.1994 | 0.2166 | 0.3745 | 0.1422 | 7.035 | -0.4122 | 2.899 |
| Semi empirical PM3 | | | | | | | | | |
| TA | 26090.366 | -0.5166 | -0.2323 | 0.2843 | 0.3745 | 0.1422 | 7.035 | -0.4122 | 6.715 |
| ATA | 87573.553 | -0.4259 | -0.2048 | 0.2211 | 0.3154 | 0.1106 | 9.042 | -0.2627 | 3.743 |
| VTA | 101122.110 | -0.4178 | -0.2067 | 0.2111 | 0.3123 | 0.1056 | 9.470 | -0.2608 | 1.991 |
| B3LYP/6 31G** | | | | | | | | | |
| TA | 221558.913 | -0.4034 | -0.2209 | 0.1825 | 0.3122 | 0.0913 | 10.953 | -0.3008 | 7.542 |
| ATA | 703229.342 | -0.3138 | -0.2134 | 0.1004 | 0.2639 | 0.0502 | 19.920 | -0.0663 | 6.491 |
| VTA | 797186.761 | 0.3035 | 0.2086 | 0.0949 | 0.2561 | 0.0475 | 21.075 | 0.0121 | 0.501 |

* -kcalmol⁻¹, ** -a.u, *** -Debye

Table 3 : Molecular volume and surface area of protonated and non-protonated inhibitors

| Molecule | Mol. vol (A3) | Surface area (A2) |
|----------------|---------------|-------------------|
| TA | 114.79 | 129.06 |
| TA_protonated | 113.22 | 128.12 |
| ATA | 401.44 | 382.97 |
| ATA_protonated | 399.88 | 383.06 |
| VTA | 420.43 | 401.17 |
| VTA_protonated | 420.13 | 401.75 |

Table 4: Calculated energy parameters for Fe-inhibitor complexes (B3LYP/6-31G//B3LYP/3-21G**)**

| Mol | Binding site | -TE ** | ΔE^* | $-E_{HOMO}^{**}$ | $-E_{LUMO}^{**}$ | ΔE^{**} | $r(Fe-C)^{***}$ | $r(Fe-N)^{***}$ |
|-----|--------------|-----------------|--------------|------------------|------------------|-----------------|-----------------|-----------------|
| TA | N1 | 1616.4092784179 | 0.0 | 0.1315 | 0.0173 | 0.1142 | - | 1.737 |
| | C3N4C5 | 1616.3956956722 | 8.5 | 0.1705 | 0.0700 | 0.1005 | 1.882 | 1.807 |
| | N1N2C3C5 | 1616.3835463374 | 16.2 | 0.1685 | 0.0654 | 0.1031 | 1.888 | 1.818 |
| ATA | N1 | 2383.7805538446 | 0.0 | 0.1308 | 0.0750 | 0.0558 | - | 1.716 |
| | C3N4C5 | 2383.7647690254 | 9.9 | 0.1836 | 0.0690 | 0.1146 | 1.895 | 1.805 |
| | N1N2C3C5 | 2383.7556490227 | 15.6 | 0.1700 | 0.0683 | 0.1017 | 1.894 | 1.836 |
| VTA | N1 | 2534.2227603708 | 0.0 | -0.1306 | -0.0744 | 0.0562 | - | 1.717 |
| | C3N4C5 | 2534.2061851996 | 10.4 | -0.1643 | -0.0769 | 0.0874 | 1.829 | 1.896 |
| | N1N2C3C5 | 2534.1979017612 | 15.6 | -0.1825 | -0.0672 | 0.1153 | 1.895 | 1.806 |

Table 5 : Calculated electrostatic potential minima of the inhibitors

| Mol | Binding site | -TE ** | ΔE^* | $-E_{HOMO}^{**}$ | $-E_{LUMO}^{**}$ | ΔE^{**} | $r(Fe-C)^{***}$ | $r(Fe-N)^{***}$ |
|-----|--------------|-----------------|--------------|------------------|------------------|-----------------|-----------------|-----------------|
| TA | N1 | 1616.4092784179 | 0.0 | 0.1315 | 0.0173 | 0.1142 | - | 1.737 |
| | C3N4C5 | 1616.3956956722 | 8.5 | 0.1705 | 0.0700 | 0.1005 | 1.882 | 1.807 |
| | N1N2C3C5 | 1616.3835463374 | 16.2 | 0.1685 | 0.0654 | 0.1031 | 1.888 | 1.818 |
| ATA | N1 | 2383.7805538446 | 0.0 | 0.1308 | 0.0750 | 0.0558 | - | 1.716 |
| | C3N4C5 | 2383.7647690254 | 9.9 | 0.1836 | 0.0690 | 0.1146 | 1.895 | 1.805 |
| | N1N2C3C5 | 2383.7556490227 | 15.6 | 0.1700 | 0.0683 | 0.1017 | 1.894 | 1.836 |
| VTA | N1 | 2534.2227603708 | 0.0 | -0.1306 | -0.0744 | 0.0562 | - | 1.717 |
| | C3N4C5 | 2534.2061851996 | 10.4 | -0.1643 | -0.0769 | 0.0874 | 1.829 | 1.896 |
| | N1N2C3C5 | 2534.1979017612 | 15.6 | -0.1825 | -0.0672 | 0.1153 | 1.895 | 1.806 |

Table 6. Calculated electrostatic potential minima of the inhibitors

| Molecule | V_{\min} values (in kcal/mol) | | | | | | | |
|----------|---------------------------------|------------|------|------------|------|------------|------|------------|
| | Atom | V_{\min} | Atom | V_{\min} | Atom | V_{\min} | Atom | V_{\min} |
| TA | N1 | -49.653 | N2 | -49.652 | N7 | -23.727 | N6 | -23.711 |
| ATA | N1 | -50.723 | N2 | -50.722 | O20 | -22.677 | O21 | -22.669 |
| VTA | N1 | 47.748 | N2 | 47.743 | O41 | 28.254 | O42 | 28.212 |

REFERENCES

- Abdelghani E., Hassan H.H. and Amin M. A., 2007. Inhibition of mild steel corrosion in hydrochloric acid solution by triazole derivatives Part I. Polarization and EIS studies. *Electrochim Acta.*, **52**:6359-6366.
- Alex A. Granovsky PC GAMESS/Firefly version 8.2.0, <http://classic.chem.msu.su/gran/gamess/index.html>
- Awad M. K., Masoud M. S., Shaker M. A. and El-Tahawy M.M. T. 2010. The role of structural chemistry in the inhibitive performance of some aminopyrimidines on the corrosion of steel. *Corros. Sci.*, **52**: 2387-2396.
- Bode B. M. and Gordon M. S., 1998. MacMolPlt: A graphical user interface for GAMESS. *Journal of Molecular Graphics and Modelling*, **16**(3):133-138.
- Gece G.; 2008. The use of quantum chemical methods in corrosion inhibitor studies *Corros Sci.*, **50**:2981-2992.
- Gopi D., Govindaraju K. M. and Kavitha L.; 2010. Investigation of Triazole derived Schiff bases as corrosion inhibitors for mild steel in hydrochloric acid medium. *J Appl Electrochem.* , **40**: 1349-1356.
- Hasanov R., Sadikoglu M. and Bilgic S., 2007. Electrochemical and quantum chemical Studies of some Schiff bases on the corrosion of steel in H₂SO₄ solution. *Appl Surf Sci.*, **253**:3913-3921.
- Jane Murray S., Tore Brinck, Pat Lane, Kim Paulsen and Peter Politzer; 1994 statistically-based interaction indices derived from molecular surface electrostatic potentials: a general interaction properties function (GIPF), *J. Mol. Struct. (THEOCHEM)*, **307**: 55-64.
- Jmol: an open-source Java viewer for chemical structures in 3D. <http://www.jmol.org/>
- Mu G. and Li X., 2005. Inhibition of cold rolled steel corrosion by Tween-20 in sulfuric acid: Weight loss, electrochemical and AFM approaches. *J Coll Interf Sci.*, **289**:184-192. Tian Lu, Feiwu Chen; 2012. Multiwfn: A Multifunctional Wavefunction Analyzer, *J Comp Chem.*, **33**: 580-592.
- Tian Lu, Feiwu Chen., 2012. Quantitative analysis of molecular surface based on Improved Marching Tetrahedra algorithm. *J Mol Graph Model.*, **38**: 314-323.

